

Original Article



Cardiotoxicity evaluation of two-drug fixed-dose combination therapy under CiPA: a computational study

Ali Ikhsanul Qauli ^{1,2}, Aroli Marcellinus ¹, Frederique Jos Vanheusden ³, and Ki Moo Lim ^{1,4,5,*}

¹Computational Medicine Lab, Department of IT Convergence Engineering, Kumoh National Institute of Technology, Gumi 39177, Korea

²Department of Engineering, Faculty of Advanced Technology and Multidiscipline, Universitas Airlangga, Surabaya 60115, Indonesia

³School of Science & Technology, Nottingham Trent University, Nottingham NG1 4FQ, United Kingdom

⁴Computational Medicine Lab, Department of Medical IT Convergence Engineering, Kumoh National Institute of Technology, Gumi 39177, Korea

⁵Meta Heart Co., Ltd., Gumi 39177, Korea

OPEN ACCESS

Received: Sep 30, 2024

Revised: Dec 17, 2024

Accepted: Dec 20, 2024

Published online: Dec 27, 2024

*Correspondence to

Ki Moo Lim

Computational Medicine Lab, Departments of IT Convergence Engineering and Medical IT Convergence Engineering, Kumoh National Institute of Technology, 61 Daehak-ro, Gumi 39177, Korea.
Email: kmlim@kumoh.ac.kr

Copyright © 2024 Translational and Clinical Pharmacology

It is identical to the Creative Commons Attribution Non-Commercial License (<https://creativecommons.org/licenses/by-nc/4.0/>).

ORCID iDs

Ali Ikhsanul Qauli

<https://orcid.org/0000-0003-4507-3812>

Aroli Marcellinus

<https://orcid.org/0009-0002-8273-6152>

Frederique Jos Vanheusden

<https://orcid.org/0000-0003-2369-6189>

Ki Moo Lim

<https://orcid.org/0000-0001-6729-8129>

Funding

This research was partially supported by the Ministry of Food and Drug Safety (22213MFDS3922 and 24212MFDS266), National Research Foundation of Korea (NRF) under the Basic Science Research Program (2022R1A2C2006326), and Ministry

ABSTRACT

The Comprehensive *In Vitro* Proarrhythmia Assay (CiPA) evaluates drug-induced torsade de pointes (TdP) risk, with qNet commonly used to classify drugs into low-, intermediate-, and high-risk categories. While most studies focus on single-drug effects, 2-drug fixed-dose combination (FDC) therapy is widely used for cardiovascular disease management.

We aimed to develop the CiPA-based methodology to predict adverse effects of FDC therapy. A human ventricular cell model was stimulated under the effects of various drug combinations from twelve well-characterized compounds suggested by CiPA at 1 to 4 maximum plasma concentration, and the qNet_{avg} biomarker as a function of the ratio of two drugs was used to evaluate the TdP risk of combined compounds. Results showed that high-risk and intermediate-risk drug combinations often yielded lower qNet_{avg} than individual drugs, suggesting increased TdP risk. Conversely, combinations involving low-risk drugs tended to reduce TdP risk by raising qNet_{avg} above individual drug levels. Also, we found that the interplay of some major ionic channels caused variations on qNet_{avg}. These findings highlight the importance of evaluating FDC cardiotoxicity to predict risks that may not appear in single-drug analysis.

Keywords: Medicine; Cardiotoxicity; Drug Interactions; Drug Polytherapy; Computer Simulation

INTRODUCTION

Torsade de pointes (TdP) is a well-known cardiac arrhythmia linked to sudden cardiac death [1]. Drug-induced TdP has become a significant concern for regulatory bodies and the pharmaceutical industries. Previously, cardiac safety assessments focused on QT interval prolongation and human ether-a-go-go-related gene (hERG) channel inhibition, per ICH E14 and S7B guidelines [2]. However, QT prolongation shows high sensitivity but low specificity in predicting ventricular arrhythmia risk, hERG channel blocking alone does

of Science and ICT Korea (MSIT) under the Grand Information Technology Research Center support program (RS-2020-II201612) supervised by the Institute for Information and Communications Technology Planning and Evaluation (IITP).

Conflict of Interest

- Authors: K.M.L. is employed by Meta Heart Inc. The other authors declare no additional conflict of interest.
- Reviewers: Nothing to declare
- Editors: Nothing to declare

Author Contributions

Formal analysis: Qauli AI; Investigation: Qauli AI; Methodology: Lim KM; Software: Qauli AI, Marcellinus A; Supervision: Lim KM; Validation: Qauli AI; Visualization: Qauli AI; Writing - original draft: Qauli AI; Writing - review & editing: Qauli AI, Marcellinus A, Vanheusden FJ, Lim KM.

not always predict action potential (AP) prolongation, and particular drugs may not pose a proarrhythmic risk but can block the hERG channel [2]. To overcome these limitations, researchers have introduced the Comprehensive *In Vitro* Proarrhythmia Assay (CiPA), which incorporates computational analysis into cardiac safety evaluations [3].

Several studies have examined the risk of TdP associated with various drugs. Mirams et al. [4] proposed using the effects of drugs on multiple ion channels to categorize TdP risk, employing the conductance-blocking model [5]. Dutta et al. [6] introduced several biomarkers for TdP risk, including qNet, which was later evaluated by Chang et al. [7] and Li et al. [8], showing qNet's effectiveness in classifying drugs by TdP risk.

Although prior studies have shown promising results, most focus on the effects of individual medicines. Yet while polypharmacy is a prevalent phenomenon in medical practice [9], evaluating the potential risks associated with drug combinations remains limited, even though international regulatory bodies, such as the European Medicines Agency, have advised the assessment of pharmacodynamic (PD) interactions in cases when multiple drugs are competing for the same target and are expected to be administered simultaneously, such as treatments that extend the QT interval [10]. Multiple investigations have documented the impact of drug-drug interactions (DDIs) on the efficacy and safety of antiarrhythmic medications when administered concurrently with antibiotics, antipsychotics, antiallergic medicines, and prokinetic agents [11-13]. Also, some studies have investigated the potential risk of TdP associated with drug combinations [14-18]. These studies evaluated the potential risk of TdP related to the combination of drugs at various doses.

Despite these advancements, drug combination studies, particularly for antiarrhythmic drugs (AADs), remain underexplored. This gap is critical given the narrow therapeutic index of AADs, where small deviations in dosage can lead to toxicity or proarrhythmic events. Additionally, AAD therapy is often complicated by adverse symptoms, organ toxicity, and proarrhythmic risks, as well as drug-drug and drug-device interactions [19]. As a result, combining 2 AADs—each at reduced doses—may improve tolerability while preserving efficacy [20]. For instance, a study demonstrated that combining low-dose quinidine with low-dose disopyramide mitigated gastrointestinal side effects observed at higher doses of either drug while maintaining their antiarrhythmic effects [21]. These examples highlight the practical relevance of AAD combinations in clinical practice.

Furthermore, the effects of drug combinations are complex and often nonlinear, particularly due to the interaction of pharmacokinetic (PK) and PD mechanisms. While the individual safety profiles of well-established AADs are well-documented, combining these drugs can result in effects that differ significantly from their individual actions. For instance, our recent study revealed nonlinear effects of drug combinations on TdP risk, even for well-characterized compounds. Specifically, combining low-risk drugs with intermediate- or high-risk drugs produced varying TdP risks depending on the concentrations of the combined drugs [22]. These findings underscore the necessity of systematically evaluating AAD combinations, including well-known compounds, to ensure safety and efficacy.

Previous studies showed that drug combinations can alter TdP risk depending on drug concentrations, but their practical application is limited without a specific combination protocol. Polypharmacy often employs one or more combinations of delivery systems, and two-drug fixed-dose combinations (FDCs) have proven more effective for treating

hypertension than monotherapy [23,24]. Hypertension is associated with the development of various atrial and ventricular arrhythmias [25-27], and since TdP is closely related to ventricular arrhythmia [1], thus with hypertension, a systematic method for evaluating the cardiotoxicity of FDC therapy is needed. With the shift of cardiac safety paradigm towards CiPA, developing the CiPA-based cardiotoxicity for FDC therapy can be one of the essential steps.

To develop CiPA-based cardiotoxicity evaluation method for 2-drug FDC, we utilized the same computational approach as our previous study [22] but focused on evaluating 2-drug FDC therapy commonly used in clinical practice. In addition, we limit the scope of this study to focus on the PD inhibition of drug combinations. We employed the Bliss independent model to predict combined drug effects (PD inhibition) using individual-drug data [28] and proposed a simulation protocol using polar coordinates for drug combinations. Additionally, we used the updated CiPA drug data from manual patch clamp experiments for *in silico* electrophysiological simulations [8].

METHODS

This section describes the model of cardiac cells and drug effects utilized in this study. Moreover, the simulation protocol to obtain the qNet average (qNet_{avg}) as a TdP metric for FDC is also described.

Model of cardiac cell

The cardiac cell model utilized in this study was from the ventricular cell model proposed by O'Hara et al. [29] that was later modified by Li et al. [30] and Dutta et al. [6]. The membrane potential (V_m) of the cardiac cell was modeled as follows:

$$\frac{dV_m}{dt} = -\frac{1}{C_m}(I_{ion} + I_{stim}) \quad (Eq. 1)$$

where the C_m is the total membrane capacitance, I_{stim} is the stimulus current, and I_{ion} is the transmembrane ionic current. The ionic transmembrane currents are assumed to consist of sodium current (I_{Na}), late sodium current (I_{NaL}), L-type calcium current (I_{CaL}), sodium current through L-type calcium channel (I_{CaNa}), potassium current through L-type calcium channel (I_{CaK}), transient outward potassium current (I_{to}), rapid delayed rectifier potassium current (I_{Kr}), slow delayed rectifier potassium current (I_{Ks}), inward rectifier potassium current (I_{K1}), sodium-potassium ATPase current (I_{NaK}), sodium-calcium exchange current (I_{NaCa}), sarcolemma calcium pump current (I_{pCa}), and background currents (I_{NaB} , I_{CaB} , I_{KB}). The maximum conductance of 5 major ionic currents (I_{Kr} , I_{Ks} , I_{K1} , I_{CaL} , and I_{NaL}) was rescaled [6].

Model of drug's effects on multiple ion channels

Each drug was assumed to inhibit seven ion channels (CaL , Na , NaL , $K1$, Ks , to , and Kr) following the Hill equation:

$$E_i = \left[1 + \left(\frac{IC50}{D} \right)^h \right]^{-1} \quad (Eq. 2)$$

where the E_i is the drug's inhibitory effect on ion channel i , D is the drug concentration (nM), $IC50$ is the 50% inhibition concentration of the drug (nM), and h is Hill's coefficient. We utilized only the conductance block expressed as Eq. 2 without the dynamic model of the hERG channel for simulating the drug's effects. Additionally, the Bliss independent model

was used to simulate the combined effects of two drugs in the FDC protocol [28]. Assuming drugs A and B act independently, their combined inhibitory effect (E_{AB}) can be calculated from the independent effects of each drug (E_A and E_B) as follows:

$$E_{AB} = E_A + E_B - E_A E_B \quad (\text{Eq. 3})$$

Each drug inhibition effect (E_A and E_B) in Eq. 3 ranges from 0 to 1. In the simulation, the inhibitory effect on each channel was converted into the “remaining” current, which was then multiplied by the ion channel conductance as follows:

$$g_i = g_{i,\text{control}}(1 - E_i) \quad (\text{Eq. 4})$$

where the $g_{i,\text{control}}$ was the maximum conductance of ion channel i without drug effect, g_i was the maximum conductance of ion channel i under drug effect, E_i was the drug's inhibitory effect on ion channel i , derived from the single or combined drug.

Simulation protocols

The overall procedure for simulation can be seen in **Fig. 1**. The first simulation (**Fig. 1A**) followed the protocol by Chang et al. [7] to assess single-drug effects. The input included IC_{50} and Hill's coefficient values for 100 samples per drug, using data from 12 CiPA drugs. IC_{50} and Hill's coefficients were obtained via nonlinear least squares fitting and Markov chain Monte Carlo simulations. The raw dose-response data and the script for calculating these values are available at <https://github.com/FDA/CiPA/tree/Model-Validation-2018>. Risk labels for each drug are shown in **Table 1**. Each single-drug simulation began with 1,000 drug-free beats to reach a steady state.

After that, the following 1,000 beats under drug's effects were simulated. Within the last 250 beats, the steady-state situation was usually achieved (as shown in **Supplementary Fig. 1**), and the beat that showed the highest maximum $\frac{dV_m}{dt}_{\text{repol}}$ during repolarization was chosen for feature extraction to depict the worst possible drug-induced adverse effects. The value of the highest maximum $\frac{dV_m}{dt}_{\text{repol}}$ was calculated from three scenarios: when the AP was fully repolarized, the maximum $\frac{dV_m}{dt}_{\text{repol}}$ was obtained between 30% and 90% repolarization; when the AP repolarized 30% but not 90%, the maximum $\frac{dV_m}{dt}_{\text{repol}}$ was calculated between 30% repolarization and the end of the beat ($t=2,000$ ms); when the AP could not repolarize by 30%, the maximum $\frac{dV_m}{dt}_{\text{repol}}$ was calculated between the AP peak and the end of the beat. Simulations were run for multiple drug concentrations (1–4× c_{max}). The qNet, introduced by Dutta et al. [6], was used to classify TdP risk, defined as the charge accumulation from six ionic currents (I_{Kr} , I_{CaL} , I_{NaL} , I_{to} , I_{Ks} , and I_{K1}) during one cycle length (CL) of an AP, expressed as follows:

$$qNet = \int_0^{CL} (I_{Kr} + I_{CaL} + I_{NaL} + I_{to} + I_{Ks} + I_{K1}) dt \quad (\text{Eq. 5})$$

The TdP metric used for classification was the average qNet across 1–4× c_{max} ($qNet_{\text{avg}}$). Ordinal logistic regression was then applied to establish $qNet_{\text{avg}}$ thresholds for classifying drugs into low, intermediate, or high-risk categories [30].

The second simulation (**Fig. 1B**) combined drugs using the FDC protocol. Input data included IC_{50} and Hill's coefficient for 2 drugs. Drug combinations were created by varying their concentrations using FDC parameters r and θ . For drugs A and B, the individual drug concentrations were expressed using polar coordinates as follows:

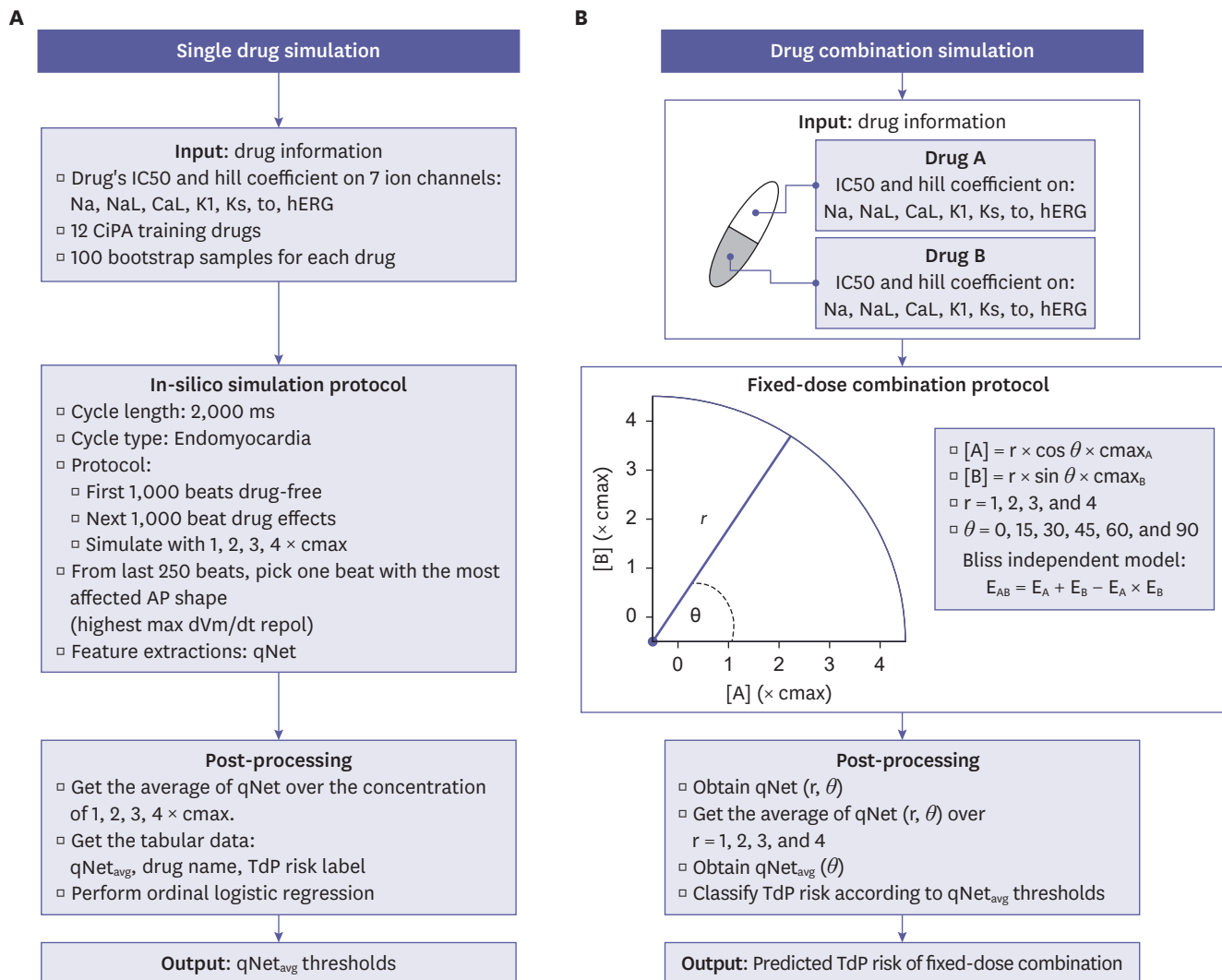


Figure 1. Protocol for in-silico simulations of the effects of a single drug and FDC. (A) The single drug simulation. Drug information, including IC50 and Hill's coefficient for seven ion channels, was used. Cell models were first stimulated 1,000 times drug-free, followed by 1,000 stimulations with the drug. The output was qNet values across several drug concentrations (1–4× cmax), and qNet_{avg} was calculated. Ordinal logistic regression then classified drugs into low, intermediate, or high-risk groups based on qNet_{avg} thresholds. (B) The FDC simulation. Inputs included IC50 and Hill's coefficient for 2 drugs, with drug ratios adjusted by parameters (r and θ). The Bliss independence model was used, and qNet_{avg}(θ) was calculated by averaging qNet_{avg}(r, θ) across different r values. The qNet_{avg}(θ) was used to assess TdP risk of the FDC based on qNet_{avg} thresholds from the single drug simulations. Further details are provided in the methods section. FDC, fixed-dose combination.

$$[A]=r \times \cos \theta \times cmax_A \quad (Eq. 6)$$

$$[B]=r \times \sin \theta \times cmax_B \quad (Eq. 7)$$

the $cmax_A$ and $cmax_B$ represent the cmax values for drugs A and B. The FDC parameters varied with $r=1,2,3,4$ and $\theta=0^\circ, 15^\circ, 30^\circ, 45^\circ, 60^\circ, 75^\circ, 90^\circ$. Here, $\theta=0^\circ$ represents drug A only, and $\theta=90^\circ$ represents drug B only. After setting the drug combinations, simulations followed the same protocol as for single drugs, producing qNet(r, θ) results. To obtain a TdP metric similar to single-drug simulations, qNet_{avg}(θ) was calculated by averaging qNet(r, θ) across r. The qNet_{avg} thresholds from the single-drug simulation were then used to classify TdP risk for the combined drugs, with 100 samples for each combination.

Table 1. The TdP risk label for each drug used in this study

Drug	C _{max} (nM)	TdP risk category
Diltiazem	122	Low
Mexiletine	4,129	Low
Ranolazine	1,948.20	Low
Verapamil	81	Low
Chlorpromazine	38	Intermediate
Cisapride	2.6	Intermediate
Terfenadine	4	Intermediate
Ondansetron	139	Intermediate
Quinidine	3,237	High
Bepridil	33	High
Dofetilide	2	High
Sotalol	14,690	High

The TdP risk labels were from CiPA's list of training drugs [6].

TdP, torsade de pointes; CiPA, Comprehensive *In Vitro* Proarrhythmia Assay.

RESULTS

The distribution of $qNet_{avg}$ for 12 CiPA drugs is shown in **Fig. 2**. The dashed lines were the $qNet_{avg}$ thresholds: $threshold_1=0.0521 \mu C/\mu F$ (red) and $threshold_2=0.0664 \mu C/\mu F$ (blue). Drugs with $qNet_{avg}$ below $threshold_1$ were categorized as high-risk, between $threshold_1$ and $threshold_2$ were classified as intermediate-risk, and above $threshold_2$ as low-risk drugs. Some drugs were classified correctly, such as quinidine, dofetilide, and diltiazem. Other drugs had their samples in several TdP classes. For example, in the high-risk drugs group, some samples of bepridil and sotalol were within intermediate and low-risk classes; in the intermediate-risk group, some samples from cisapride and terfenadine were in intermediate and high-risk regions, while some samples from chlorpromazine and ondansetron were in intermediate and low-risk region; in low-risk drugs group, some samples from mexiletine, ranolazine, and verapamil were categorized as either low or intermediate.

Fig. 3 shows drug combination plots of twelve CiPA drugs. Each plot represents the $qNet_{avg}(\theta)$ of the combined drugs with red, blue, and green regions represent TdP risk. The horizontal black dashed line represents the drug-free result ($qNet_{avg}=0.072 \mu C/\mu F$). The white region shows the variation of $qNet_{avg}$, and the black line indicates the mean value. Combinations with quinidine and dofetilide mostly fell in the high- and intermediate-risk areas. At $\theta=0^\circ$ or $\theta=90^\circ$, $qNet_{avg}$ values matched those from single-drug simulations, consistent with **Fig. 2** results.

Overall, combinations of high-risk drugs mostly showed high-risk results. However, some combinations involving bepridil and sotalol also had compounds in the low- and intermediate-risk regions. Most combinations resulted in lower $qNet_{avg}$ values than their single-dose drugs, as seen with quinidine-dofetilide, quinidine-sotalol, and bepridil-dofetilide pairs. Similarly, combinations of intermediate-risk drugs showed lower $qNet_{avg}$ values, but some low-risk drug pairs, like mexiletine-diltiazem, resulted in higher $qNet_{avg}$.

Combinations of high and intermediate-risk drugs were mostly in the high- and intermediate-risk regions. However, some had low-risk samples, like sotalol-ondansetron, sotalol-chlorpromazine, and combinations incorporating bepridil. High and low-risk drug combinations could also produce low-risk $qNet_{avg}$, especially those with bepridil or sotalol, except for sotalol-ranolazine and sotalol-verapamil. Finally, some intermediate and low-risk combinations, like chlorpromazine-verapamil, had higher $qNet_{avg}$ than their single-dose drugs.

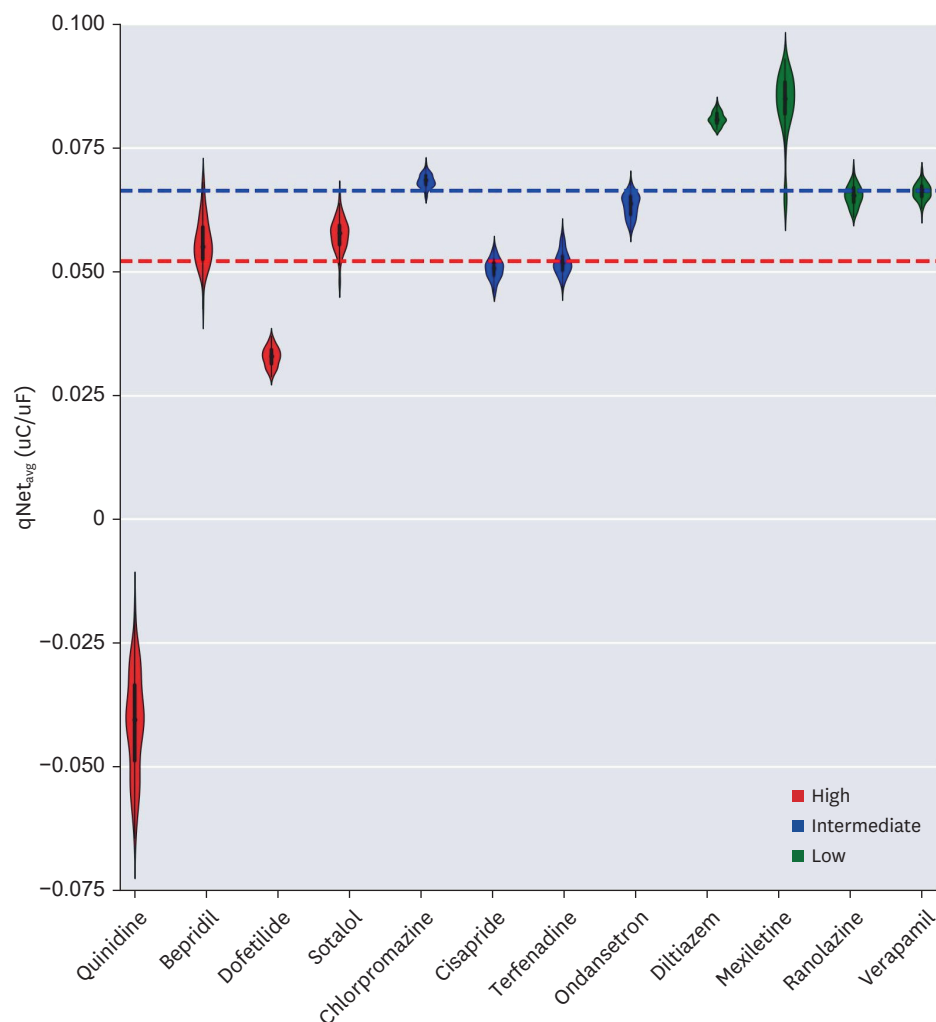


Figure 2. $qNet_{avg}$ distribution for 12 CiPA drugs (single drug effects) is shown with color coding for TdP risk: red for high-risk, blue for intermediate-risk, and green for low-risk. The horizontal dashed lines represent $qNet_{avg}$ thresholds: red for $threshold_1=0.0521 \mu C/\mu F$ and blue for $threshold_2=0.0664 \mu C/\mu F$. Samples with $qNet_{avg}$ below $threshold_1$ were categorized as high-risk, between $threshold_1$ and $threshold_2$ as intermediate-risk, and above $threshold_2$ as low-risk samples.

CiPA, Comprehensive *In Vitro* Proarrhythmia Assay; TdP, torsade de pointes.

Furthermore, to assess whether a drug pair increases or decreases $qNet_{avg}$ relative to single-dose drugs, the minimum or maximum $qNet_{avg}$ values were evaluated based on the drug ratio (θ). **Table 2** shows where minimum and maximum $qNet_{avg}$ occurred. Drug pairs with $qNet_{avg}$ values lower or higher than single-dose drugs can indicate potential changes in TdP risk, especially at θ values other than 0° or 90° . From the number of samples shown at $\theta=15^\circ, 30^\circ, 45^\circ, 60^\circ, 75^\circ$, one can predict the portion of drug samples with higher or lower TdP risk than their single-dose drugs.

Within high-risk drug pairs, only the pair of quinidine-bepridil showed the lowest $qNet_{avg}$ at $\theta=0^\circ$, meaning quinidine alone produced the lowest value. The highest $qNet_{avg}$ occurred at $\theta=0^\circ$ or $\theta=90^\circ$, indicating single-dose drugs generated these values. As a consequence, all high-risk drug combinations had a high probability of increasing TdP risk, with quinidine-sotalol at 80% as the least and dofetilide-sotalol at 100% as the highest. Finally, none of these combinations reduced TdP risk compared to single-dose drugs.

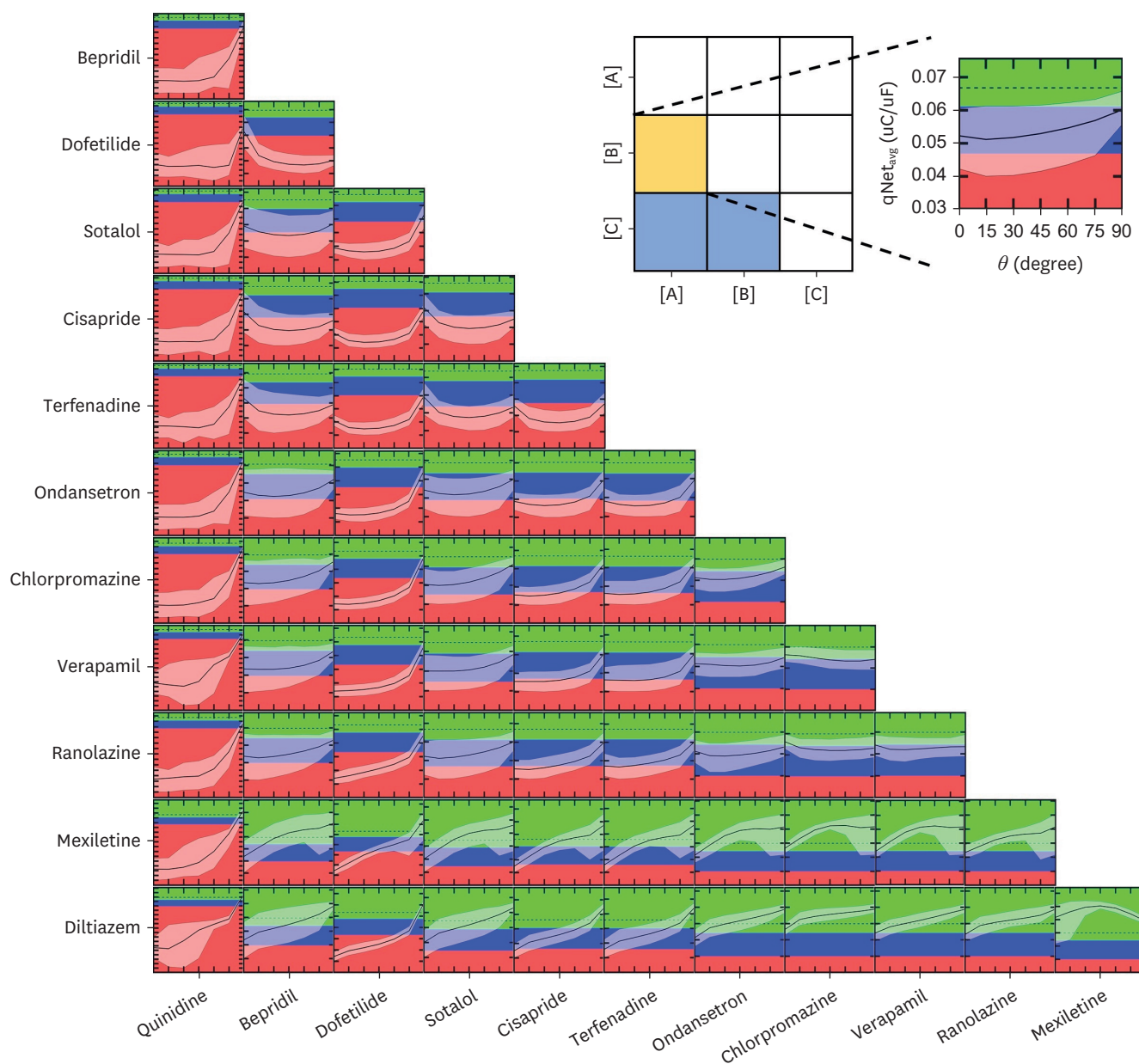


Figure 3. Drug combination plots for TdP risk predictions are shown for 66 possible combinations of 12 CiPA drugs. Each plot displays the variation of $qNet_{avg}(\theta)$ for the combined compounds, with red, blue, and green areas representing TdP risk regions. The horizontal black dashed line indicates the drug-free simulation result ($qNet_{avg}=0.072 \mu C/\mu F$). The black line represents the mean $qNet_{avg}(\theta)$, while the transparent white region shows variations from 100 samples. TdP, torsade de pointes; CiPA, Comprehensive *In Vitro* Proarrhythmia Assay.

For high- and intermediate-risk drug pairs, the lowest $qNet_{avg}$ mostly appeared at θ other than 0° or 90° , suggesting higher TdP risk than single-dose drugs. Exceptions were bepridil-chlorpromazine, quinidine-chlorpromazine, and quinidine-ondansetron, which had $qNet_{avg}$ at $\theta=0^\circ$, showing no increased risk. Some pairs, like bepridil-cisapride, bepridil-terfenadine, sotalol-cisapride, and sotalol-terfenadine, had the highest $qNet_{avg}$ at $\theta=0^\circ$, bepridil-ondansetron at $\theta=30^\circ$, while others were at $\theta=90^\circ$. All 16 combinations showed increased TdP risk, with dofetilide-chlorpromazine being the lowest at 72%, and several pairs, including dofetilide-cisapride, dofetilide-terfenadine, sotalol-cisapride, sotalol-terfenadine, and

Table 2. The drug ratio (θ) where the lowest or highest $qNet_{avg}$ occurs for all drug samples reflects their tendency to increase or decrease TdP risk in combination

Label	Drug		θ at minimum $qNet_{avg}$							θ at maximum $qNet_{avg}$							Combined TdP risk		
	A	B	0°	15°	30°	45°	60°	75°	90°	0°	15°	30°	45°	60°	75°	90°	Increases	Decreases	
High-high	bepridil	dofetilide	0	0	0	16	70.8*	5.83	7.33	100†	0	0	0	0	0	0	93%	0%	
	bepridil	sotalol	0	1	22.5	65.5*	4	0.5	6.5	41.5†	0	0	0	0	0	58.5	94%	0%	
	dofetilide	sotalol	0	8.5	79*	12.5	0	0	0	0	0	0	0	0	0	100†	100%	0%	
	quinidine	bepridil	16.8*	19.3	23.8	38	2	0	0	0	0	0	0	0	0	100†	83%	0%	
	quinidine	dofetilide	7	13.5	12	30.5	12*	25	0	0	0	0	0	0	0	100†	93%	0%	
	quinidine	sotalol	20.5	13	19.5	42	5*	0	0	0	0	0	0	0	0	100†	80%	0%	
	High-intermediate	bepridil	cisapride	0	0	6*	80.5	5.5	0.5	7.5	87.5†	0	0	0	0	0	12.5	93%	0%
		bepridil	terfenadine	0	0	12*	77.8	2.83	0	7.33	76.5†	0	0	0	0	0	23.5	93%	0%
		bepridil	ondansetron	1.5	15.5	58.8*	20.8	0	0	3.33	10.5	0	0.5†	0.5	0.5	87.5	95%	2%	
		bepridil	chlorpromazine	18.5*	71	10.5	0	0	0	0	1	0	0	0	2.33	3.33	93.3†	82%	6%
dofetilide		cisapride	0	0	73.5*	26.5	0	0	0	0	0	0	0	0	0	100†	100%	0%	
dofetilide		terfenadine	0	1	84*	15	0	0	0	0	0	0	0	0	0	100†	100%	0%	
dofetilide		ondansetron	8	57.5	33.5*	1	0	0	0	0	0	0	0	0	0	100†	92%	0%	
dofetilide		chlorpromazine	28	70*	1	1	0	0	0	0	0	0	0	0	0	100†	72%	0%	
quinidine		cisapride	12.5	25	14.5	36	11*	1	0	0	0	0	0	0	0	100†	88%	0%	
quinidine		terfenadine	12.5	13.5	21*	44	9	0	0	0	0	0	0	0	0	100†	88%	0%	
High-low	quinidine	ondansetron	20*	16	26	37	1	0	0	0	0	0	0	0	0	100†	80%	0%	
	quinidine	chlorpromazine	17.5*	14.5	32	36	0	0	0	0	0	0	0	0	0	100†	83%	0%	
	sotalol	cisapride	0	0	4.5	82.5	12.5	0.5	0	96†	0	0	0	0	0	4	100%	0%	
	sotalol	terfenadine	0	0	11	79.5*	9	0.5	0	91.5†	0	0	0	0	0	8.5	100%	0%	
	sotalol	ondansetron	0.5	10.5	68.5	20*	0.5	0	0	7	0	0	0	0	0	93†	100%	0%	
	sotalol	chlorpromazine	14.5	73*	12	0.5	0	0	0	0	0	0	0	0	0	100†	86%	0%	
	bepridil	verapamil	36.2*	18.7	36.2	7	0	0.5	1.5	1	0	0	2	1.5	2.5	93†	62%	6%	
	bepridil	ranolazine	27.3	61.3*	8.83	0.5	0	0	2	5	0	0.5	0	0.5	1.5	92.5†	71%	3%	
	bepridil	mexiletine	100*	0	0	0	0	0	0	0	0	0	6.5	9	2.5	82†	0%	18%	
	bepridil	diltiazem	100*	0	0	0	0	0	0	0	0	0	0	0.33	3.33	96.3†	0%	4%	
High-low	dofetilide	verapamil	73.5*	22.5	3	1	0	0	0	0	0	0	0	0	0	100†	27%	0%	
	dofetilide	ranolazine	89*	11	0	0	0	0	0	0	0	0	0	0	0	100†	11%	0%	
	dofetilide	mexiletine	100*	0	0	0	0	0	0	0	0	0	0	0	0	100†	0%	0%	
	dofetilide	diltiazem	100*	0	0	0	0	0	0	0	0	0	0	0	0	100†	0%	0%	
	quinidine	verapamil	17	21	37*	25	0	0	0	0	0	0	0	0	0	100†	83%	0%	
	quinidine	ranolazine	39	15.5*	6.5	33	6	0	0	0	0	0	0	0	0	100†	61%	0%	
	quinidine	mexiletine	31*	29	30	10	0	0	0	0	0	0	0	0	0	100†	69%	0%	
	quinidine	diltiazem	30	46	23*	1	0	0	0	0	0	0	0	0	0	100†	70%	0%	
	sotalol	verapamil	44.7*	18.2	29.5	7.33	0.33	0	0	0	0	0	0	0	0	100†	55%	0%	
	sotalol	ranolazine	23	64.5*	12	0.5	0	0	0	1	0	0	0	0	0	99†	77%	0%	
sotalol	mexiletine	100*	0	0	0	0	0	0	0	0	0	9	4	1	86†	0%	14%		
sotalol	diltiazem	100*	0	0	0	0	0	0	0	0	0	0	0	0	100†	0%	0%		

(continued to the next page)

Table 2. (Continued) The drug ratio (θ) where the lowest or highest $qNet_{avg}$ occurs for all drug samples reflects their tendency to increase or decrease TdP risk in combination

Label	Drug		θ at minimum $qNet_{avg}$						θ at maximum $qNet_{avg}$						Combined TdP risk			
	A	B	0°	15°	30°	45°	60°	75°	90°	0°	15°	30°	45°	60°	75°	90°	Increases	Decreases
Intermediate-intermediate	terfenadine	terfenadine	0	0	13.5	82.5*	4	0	0	37	0	0	0	0	0	63†	100%	0%
	cisapride	ondansetron	2.33	7.67	74.2*	15.8	0	0	0	0	0	0	0	0	0	100†	98%	0%
	cisapride	chlorpromazine	13.8	71.3*	14.8	0	0	0	0	0	0	0	0	0	0	100†	86%	0%
	ondansetron	chlorpromazine	9.83	34.8*	48.8	6.5	0	0	0	3	0	0	0	0	0	97†	90%	0%
	terfenadine	ondansetron	1.33	5.33	57.8*	35.5	0	0	0	0	0	0	0	0	0	100†	99%	0%
	terfenadine	chlorpromazine	15.8	61.2	22.7*	0.33	0	0	0	0	0	0	0	0	0	100†	84%	0%
	chlorpromazine	verapamil	3	0	0	4.5	45.2	39.2	8.17	64.3	25.8†	0.2	0.2	0.2	0.2	9.03	89%	27%
	chlorpromazine	ranolazine	3	6.83	14.8	28.8*	30.5	12.8	3.25	83.5†	3	0	0	0	0	13.5	94%	3%
	chlorpromazine	mexiletine	92	0	0	0	0	8*	0	0	0	0	38.3	7.83	1.5	52.3†	8%	48%
	chlorpromazine	diltiazem	100†	0	0	0	0	0	0	0	0	0	0.25	0.25	0.75	98.8†	0%	1%
Intermediate-low	cisapride	verapamil	43.8*	15.3	36.3	4.5	0	0	0	0	0	0	0	0	0	100†	56%	0%
	cisapride	ranolazine	37.5	59.8*	2.33	0.33	0	0	0	0	0	0	0	0	0	100†	63%	0%
	cisapride	mexiletine	100†	0	0	0	0	0	0	0	0	4	4	0	0	92†	0%	8%
	cisapride	diltiazem	100†	0	0	0	0	0	0	0	0	0	0	0	0	100†	0%	0%
	ondansetron	verapamil	18.7	2.17*	15.3	45.7	17.2	1	0	14	3.5	0	0	0	0	82.5†	81%	4%
	ondansetron	ranolazine	12.8	32.5*	37.5	13.2	4	0	0	27	0	0	0	0	0	73†	87%	0%
	ondansetron	mexiletine	94*	0	0	0	0	6	0	0	0	0	20	2	0.5	77.5†	6%	23%
	ondansetron	diltiazem	100†	0	0	0	0	0	0	0	0	0	0	0	0	100†	0%	0%
	terfenadine	verapamil	33.8	10.8*	40.3	15	0	0	0	0	0	0	0	0	0	100†	66%	0%
	terfenadine	ranolazine	35.5	59*	4.5	1	0	0	0	0	0	0	0	0	0	100†	65%	0%
Low-low	terfenadine	mexiletine	100†	0	0	0	0	0	0	0	0	5.5	2.5	0	0	92†	0%	8%
	terfenadine	diltiazem	100†	0	0	0	0	0	0	0	0	0	0	0	0	100†	0%	0%
	mexiletine	diltiazem	19*	0	0	0	0	0	81	0	8.5	25.5†	64	2	0	0	0%	100%
	ranolazine	mexiletine	92	0	0	0	0	8*	0	0	0	11.5	0	0	0	88.5†	8%	12%
	ranolazine	diltiazem	100†	0	0	0	0	0	0	0	0	0	0	0	4.5	95.5†	0%	5%
	verapamil	ranolazine	9.5	33	25.5*	9.83	1.83	2.17	18.2	55.8	5	0.5	0	0.5	10.3	27.8†	72%	16%
	verapamil	mexiletine	93*	0	0	0	0	5.5	1.5	0	0	0	27.3	13.8	9	49.8†	6%	50%
	verapamil	diltiazem	100†	0	0	0	0	0	0	0	0	0	0	0	1	99†	0%	1%

The numbers at each θ show how many samples have minimum or maximum $qNet_{avg}$. On the right, the proportion of drug samples with higher or lower combined TdP risk compared to single-dose drugs is calculated by summing samples with minimum or maximum $qNet_{avg}$ at $\theta=15^\circ, 30^\circ, 45^\circ, 60^\circ, 75^\circ$ and dividing by the total number of samples (100). Shaded cells represent non-zero values, with a color scale from 0 (white) to 100 (dark grey).

TdP, torsade de pointes.
An asterisk (*) marks the θ with the lowest $qNet_{avg}$, and a dagger (†) indicates the highest.

sotalol-ondansetron, showing 100% higher risk. However, there was a slight chance of reduced TdP risk for pairs like bepridil-ondansetron (2%) and bepridil-chlorpromazine (6%).

In high- and low-risk drug pairs, the lowest $qNet_{avg}$ mainly occurred at $\theta=0^\circ$, except for a few pairs like bepridil-ranolazine ($\theta=15^\circ$), quinidine-diltiazem ($\theta=30^\circ$), quinidine-ranolazine ($\theta=15^\circ$), quinidine-verapamil ($\theta=30^\circ$), and sotalol-ranolazine ($\theta=15^\circ$). Six pairs, including bepridil-mexiletine, bepridil-diltiazem, dofetilide-mexiletine, dofetilide-diltiazem, sotalol-mexiletine, and sotalol-diltiazem, showed 0% increased TdP risk, indicating stronger effects from the high-risk drugs (bepridil, dofetilide, and sotalol). The highest $qNet_{avg}$ for high- and low-risk drug pairs was at $\theta=90^\circ$, falling in the low-risk range. Most pairs had no reduced TdP risk, except bepridil-verapamil (6%), bepridil-ranolazine (3%), bepridil-mexiletine (18%), bepridil-diltiazem (4%), and sotalol-mexiletine (14%).

Moreover, the combinations of both intermediate-risk drugs showed the lowest values of $qNet_{avg}$ at $\theta=15^\circ$ (cisapride-chlorpromazine and ondansetron-chlorpromazine), $\theta=30^\circ$ (cisapride-ondansetron, terfenadine-ondansetron, and terfenadine-chlorpromazine), and $\theta=45^\circ$ (cisapride-ondansetron), whereas the highest values of $qNet_{avg}$ were yielded only at $\theta=90^\circ$. As a consequence, all drug pairs showed higher TdP risk than the single-dose drugs, with the least probability being 84% (terfenadine-chlorpromazine) and the highest one being 100% (cisapride-terfenadine).

For intermediate and low-risk drug combinations, pairs with diltiazem or mexiletine showed the lowest $qNet_{avg}$ at $\theta=0^\circ$, except chlorpromazine-mexiletine ($\theta=75^\circ$). Consequently, most pairs with diltiazem or mexiletine had a 0% probability of higher TdP risk compared to single-dose drugs, except chlorpromazine-mexiletine (8%) and ondansetron-mexiletine (6%). Other pairs in this group showed higher TdP risk, with probabilities ranging from 56% (cisapride-verapamil) to 94% (chlorpromazine-ranolazine). Interestingly, eight pairs showed potential for lower TdP risk than single-dose drugs, with the highest probability seen in chlorpromazine-mexiletine (48%), followed by chlorpromazine-verapamil (27%), ondansetron-mexiletine (23%), terfenadine-mexiletine (8%), cisapride-mexiletine (8%), ondansetron-verapamil (4%), chlorpromazine-ranolazine (3%), and chlorpromazine-diltiazem (1%).

Furthermore, the pairs of both low-risk drugs yielded lowest $qNet_{avg}$ mostly at $\theta=0^\circ$ except for ranolazine-mexiletine ($\theta=75^\circ$) and verapamil-ranolazine ($\theta=30^\circ$). As a consequence, most drug pairs showed no increased TdP risk compared to single-dose drugs except for pairs of verapamil-ranolazine (72%), ranolazine-mexiletine (8%), and verapamil-mexiletine (6%). Additionally, all pairs showed lower TdP risk than single-dose drugs, with the lowest possibility shown by verapamil-diltiazem (1%) and the highest yielded by mexiletine-diltiazem (100%).

DISCUSSION

This study examined the 2-drug FDC protocol using computational assessment within the CiPA framework. The cardiac cell model from O'Hara et al. [29], modified by Li et al. [30] and Dutta et al. [6], was used without dynamic models of the hERG or K_r channels. The Bliss independent model simulated the combined drug effects, adjusting FDC parameters (r and θ) to calculate various $qNet$ values. Using $qNet_{avg}$ (average $qNet$ across $r=1,2,3,4$) as the TdP risk

metric, drug combinations were classified based on single-drug $qNet_{avg}$ thresholds [7,8]. The maximum and minimum $qNet_{avg}$ values were used to assess the FDC's nonlinear impact on TdP risk.

The single drug results in **Fig. 2** show discrepancies compared to **Fig. 2** from Li et al. [8], likely due to differences in cell and drug models (detailed in **Supplementary Tables 1 and 2**). In **Fig. 2**, bepridil had higher $qNet_{avg}$ than dofetilide, while in Li et al. [8], bepridil showed lower $qNet$ values, possibly due to its weaker *Kr* channel blocking effect (35%) compared to dofetilide's 67% (**Supplementary Data 1, Supplementary Figs. 1-9**).

Although $qNet_{avg}$ thresholds in **Fig. 2** are similar to those in Li et al. [8], differences in $qNet_{avg}$ distribution affect classification performance. Without the dynamic *Kr* model, our performance is expected to be lower than the CiPAORdv1 model (as detailed in **Supplementary Table 2**), which incorporates dynamic hERG characteristics but is harder to implement for DDIs study [8]. Despite these differences, the cell model in this study closely matches CiPAORdv1 physiologically, as shown in **Supplementary Figs. 1 and 2**. In contrast, a recent cell model proposed by Tomek et al. [31] failed to reach steady-state (**Supplementary Data 1 and Supplementary Fig. 3**). Therefore, the single-drug simulations here are consistent with previous studies and suitable for analyzing 2-drug FDC therapy.

Furthermore, the single drug effects on $qNet_{avg}$ in **Fig. 2** offer insights into the nonlinear variations of $qNet_{avg}(\theta)$ in FDC simulations (**Fig. 3**). All high-risk drugs had minimum $qNet_{avg}$ values in the high-risk region (**Fig. 2**), and most drug combinations incorporating high-risk drugs showed similar results, especially when θ was close to 0° or 90° (**Fig. 3**). For example, combinations incorporating quinidine or dofetilide showed a strong tendency to be high-risk as $qNet_{avg}$ dropped around θ up to 75° .

However, combinations comprising bepridil or sotalol showed a weaker tendency to generate low $qNet_{avg}$ compared to quinidine or dofetilide, especially when paired with low-risk drugs like mexiletine or diltiazem (**Fig. 3**). This aligns with **Fig. 2**, where bepridil and sotalol also had samples in intermediate and low-risk regions. Similarly, from **Fig. 3**, drug combinations involving low-risk drugs such as mexiletine or diltiazem consistently yielded $qNet_{avg}$ in the low-risk region, presumably because the most samples from mexiletine or diltiazem are within the low-risk region (**Fig. 2**). In contrast, also from **Fig. 3**, combinations with other low-risk drugs (ranolazine or verapamil) showed differently with $qNet_{avg}$ in intermediate-risk regions. Again, these results align with single-drug results in **Fig. 2** that some big portions of ranolazine and verapamil samples are within intermediate-risk region, causing more combinations yielding intermediate-risk responses.

Furthermore, as shown in **Table 2**, some drug combinations resulted in lower or higher $qNet_{avg}$ than their single-dose drugs, indicating changes in TdP risk. All combinations of both high-risk, high- and intermediate-risk, and both intermediate-risk drugs had possibilities of yielding lower $qNet_{avg}$ (increased TdP risk). Among high- and low-risk drug combinations, 10 out of 16 pairs showed potential for lower $qNet_{avg}$. Additionally, 3 out of 6 low-risk drug pairs also showed a similar trend, with verapamil-ranolazine having a high probability (73%) and ranolazine-mexiletine and verapamil-mexiletine showing smaller probabilities (8% and 6%, respectively).

Drug combinations resulting in higher $qNet_{avg}$ (decreased TdP risk) than single-dose drugs were rare and occurred only in a few cases: high- and intermediate-risk (2 out of 16 pairs),

high- and low-risk (5 out of 16 pairs), intermediate- and low-risk (8 out of 16 pairs), and all low-risk combinations (6 out of 6 pairs). No such tendency was observed in combinations of both high- or intermediate-risk drugs. However, when high- or intermediate-risk drugs were combined with low-risk drugs, the likelihood of higher $qNet_{avg}$ increased (**Table 2**). Among low-risk drug pairs, only mexiletine-diltiazem (100%) and verapamil-mexiletine (50%) showed higher $qNet_{avg}$ with more than 50% probability. These results align with the sensitivity analysis in **Supplementary Fig. 4**, which highlights the significant role of the *CaL*, *Kr*, *Na*, and *NaL* channels in influencing $qNet_{avg}$ and TdP risk. For example, the bepridil-ondansetron pair shows dominant blocking of *CaL* and *NaL* channels (**Supplementary Fig. 6**), consistent with findings that blocking these channels raises $qNet_{avg}$ while blocking *Kr* and *Na* channels tends to lower it (**Supplementary Fig. 4**). Similar trends were observed for other drug pairs, such as bepridil-chlorpromazine, particularly at $\theta=60^\circ, 75^\circ, 90^\circ$. Other detailed results showing $qNet_{avg}$ higher than single-dose drugs are presented in **Supplementary Figs. 7-9**.

Furthermore, results from previous studies were compared for validation, as shown in **Fig. 3** and **Table 2**. Some research examined several drug combinations, including diltiazem-verapamil and diltiazem-ondansetron [32,33]. The authors reported that diltiazem was able to induce myocardial infarction and ventricular tachycardia; ondansetron could cause myocardial infarction, ventricular tachycardia, and hypertension; and verapamil could induce myocardial infarction, ischemic stroke, ventricular tachycardia, and cardiac failure [32]. Furthermore, a combination of diltiazem-verapamil could potentially induce myocardial infarction, whereas the pair of diltiazem and ondansetron had a low possibility of causing ischemic stroke [33]. These results could indicate that the corresponding drug pairs might not yield adverse drug effects other than those from their single-dose drugs. We found consistent results in the previous study that diltiazem-verapamil showed no tendency to generate higher TdP risk but a small possibility (1%) for yielding a lower TdP risk. In contrast, the diltiazem-ondansetron showed no tendency towards both increasing or decreasing the TdP risk.

Although the predictive capability of showing changes in TdP risk of drug combinations is evident, this study has several limitations. DDI is a complex phenomenon that may require a more realistic model than the Bliss independent model, such as a general PD interaction model, to produce more accurate outcomes [34]. The Bliss independent model assumes that the compounds act independently and have different modes of action; therefore, it cannot show statistical inference on synergistic effects [28,35]. On the one hand, the CiPA standard cardiac cell model (CiPAORdv1.0) includes the dynamic inhibition PD model for the hERG channel. On the other hand, the Bliss independent model only combines the steady-state effects of combined drugs, making it challenging for predicting the cardiotoxicity of FDC therapy using the CiPAORdv1.0 model [8]. When the experimental data is sufficient, the general PD interaction model can be applied for a more realistic prediction of TdP risk of FDC therapy [34].

In addition, while the current study primarily focuses on PD interactions, PK interactions, such as those influencing drug absorption, distribution, metabolism, or excretion, were not explicitly incorporated. As highlighted by Benet [36], PK DDIs can significantly alter drug concentrations in the body, which may result in unintended toxicity or therapeutic failure. For example, quinidine combined with verapamil or diltiazem has been shown to elevate plasma quinidine concentrations, necessitating monitoring for quinidine toxicity [37-41]. Dofetilide combined with verapamil can increase plasma concentration of dofetilide, therefore should be avoided in patients administered with dofetilide [42]. Similarly, the combination of quinidine and mexiletine increases serum mexiletine concentrations due

to CYP2D6 inhibition, leading to a heightened risk of mexiletine-related adverse effects [43,44]. PK interactions are also particularly important for AADs, which often rely on narrow therapeutic windows and share metabolic pathways, making them susceptible to clinically significant interactions. Future research integrating PK and PD models would provide a more comprehensive and clinically realistic assessment of drug combination effects, improving predictions of TdP risk.

Furthermore, the effect of inter-individual variability on the physiological properties of the population is not considered in this study. Variations in physiological properties, such as ion channel conductance, can alter the TdP risk of drugs [45]. Incorporating inter-individual variability through virtual populations in the cardiotoxicity evaluation of FDC therapy may offer more comprehensive insights by combining two sources of variability: the drug samples and individuals.

SUPPLEMENTARY MATERIALS

Supplementary Data 1

Supplementary materials

Supplementary Table 1

Comparison of simulation protocol for single drug analysis between this study and previous research

Supplementary Table 2

The classification performance of the single-drug evaluation

Supplementary Figure 1

Steady-state analysis of ORd model [S1,S2] with optimized ion channels' conductances. (A) The profile of Na_i from *in silico* simulations for 1–1,000 beats. (B) Graph shows the absolute error (difference in values of data point) between the Na_i profile relative to Na_i profile at the first beat. (C) The sum of absolute error for each beat in panel B. (D) The relative error between the consecutive sum of absolute error from panel C.

Supplementary Figure 2

Steady-state analysis of CiPAORdv1 model [S2,S3]. The descriptions of each panel are the same as in **Supplementary Fig. 1**.

Supplementary Figure 3

Steady-state analysis of Tomek model [S4]. The descriptions of each panel are the same as in **Supplementary Fig. 1**. Additionally, the arrows in (A, B) represent the variation number of beats from small to high (maximum is 10,000 beats).

Supplementary Figure 4

The effect of ion channel perturbation by -10% and $+10\%$ to $qNet_{avg}$. The perturbation is done by varying one ion channel while other channels are fixed. The black bar is the $qNet_{avg}$ under drug-free (control) conditions.

Supplementary Figure 5

The averaged blocking effects under drug concentration of $1-4 \times c_{max}$ of 12 training drugs from CiPA on seven ion channels (*CaL*, *KI*, *Ks*, *Na*, *NaL*, and hERG). The box plots in the figure represent the distribution of blocking effects. In one box plot, the small circles represent outliers; the top and bottom horizontal lines are the maximum and minimum values excluding outliers; the upper, middle, and lower lines in the box are the third quartile, median, and first quartile.

Supplementary Figure 6

The averaged blocking effects over radius 1–4 of some of the 2-drug FDC pairs of high- and intermediate-risk drugs on seven ion channels (*CaL*, *KI*, *Kr*, *Na*, *NaL*, and *to*) as varying θ . The drug combinations shown are the combinations that can decrease the TdP risk lower than single-dose drugs'. (A) represents the results of one drug sample from the combination of bepridil and ondansetron, and (B) is from the combination of bepridil and chlorpromazine. The bar plots represent the inhibition effects (in %) on seven ion channels, whereas the corresponding $qNet_{avg}$ values are represented by the line plot (secondary left vertical axis). Please note that the drug sample on every panel is not necessarily the same.

Supplementary Figure 7

The averaged blocking effects over radius 1–4 of some 2-drug FDC pairs of high- and low-risk drugs on seven ion channels (*CaL*, *KI*, *Kr*, *Na*, *NaL*, and *to*) as varying θ . The drug combinations shown are the combinations that can decrease the TdP risk lower than single-dose drugs. Each panels represent results of one drug sample from combinations of (A) bepridil-verapamil, (B) bepridil-ranolazine, (C) bepridil-mexiletine, (D) bepridil-diltiazem, and (E) sotalol-mexiletine, respectively. Please note that the description of the bar and line plots in the figure is the same as in **Supplementary Fig. 6**.

Supplementary Figure 8

The averaged blocking effects over radius 1–4 of some 2-drug FDC pairs of intermediate- and low-risk drugs on seven ion channels (*CaL*, *KI*, *Kr*, *Na*, *NaL*, and *to*) as varying θ . The drug combinations shown are the combinations that can decrease the TdP risk lower than single-dose drugs. Each panels represent results of one drug sample from combinations of (A) chlorpromazine-verapamil, (B) chlorpromazine-ranolazine, (C) chlorpromazine-mexiletine, (D) chlorpromazine-diltiazem, (E) cisapride-mexiletine, (F) ondansetron-verapamil, (G) ondansetron-mexiletine, and (H) terfenadine-mexiletine, respectively. Please note that the description of the bar and line plots in the figure is the same as in **Supplementary Fig. 6**.

Supplementary Figure 9

The averaged blocking effects over radius 1–4 of some of 2-drug FDC pairs of both low-risk drugs on seven ion channels (*CaL*, *KI*, *Kr*, *Na*, *NaL*, and *to*) as varying θ . The drug combinations shown are the combinations that can decrease the TdP risk lower than single-dose drugs. Each panels represent results of one drug samples from combinations of (A) mexiletine-diltiazem, (B) ranolazine-mexiletine, (C) ranolazine-diltiazem, (D) verapamil-ranolazine, (E) verapamil-mexiletine, and (F) verapamil-diltiazem, respectively Please note that the description of the bar and line plots in the figure is the same as in **Supplementary Fig. 6**.

REFERENCES

1. Drew BJ, Ackerman MJ, Funk M, Gibler WB, Kligfield P, Menon V, et al. Prevention of torsade de pointes in hospital settings: a scientific statement from the American Heart Association and the American College of Cardiology Foundation. *Circulation* 2010;121:1047-1060. [PUBMED](#) | [CROSSREF](#)
2. Sager PT, Gintant G, Turner JR, Pettit S, Stockbridge N. Rechanneling the cardiac proarrhythmia safety paradigm: a meeting report from the Cardiac Safety Research Consortium. *Am Heart J* 2014;167:292-300. Available from: <https://doi.org/10.1016/j.ahj.2013.11.004> [PUBMED](#) | [CROSSREF](#)
3. Strauss DG, Gintant G, Li Z, Wu W, Blinova K, Vicente J, et al. Comprehensive *In Vitro* Proarrhythmia Assay (CiPA) update from a Cardiac Safety Research Consortium/Health and Environmental Sciences Institute/FDA Meeting. *Ther Innov Regul Sci* 2019;53:519-525. [PUBMED](#) | [CROSSREF](#)
4. Mirams GR, Cui Y, Sher A, Fink M, Cooper J, Heath BM, et al. Simulation of multiple ion channel block provides improved early prediction of compounds' clinical torsadogenic risk. *Cardiovasc Res* 2011;91:53-61. [PUBMED](#) | [CROSSREF](#)
5. Hill AV. The possible effects of the aggregation of the molecules of haemoglobin on its dissociation curves. *J Physiol* 1910;40:i-vii. [CROSSREF](#)
6. Dutta S, Chang KC, Beattie KA, Sheng J, Tran PN, Wu WW, et al. Optimization of an *in silico* cardiac cell model for proarrhythmia risk assessment. *Front Physiol* 2017;8:616. [PUBMED](#) | [CROSSREF](#)
7. Chang KC, Dutta S, Mirams GR, Beattie KA, Sheng J, Tran PN, et al. Uncertainty quantification reveals the importance of data variability and experimental design considerations for *in silico* proarrhythmia risk assessment. *Front Physiol* 2017;8:917. [PUBMED](#) | [CROSSREF](#)
8. Li Z, Ridder BJ, Han X, Wu WW, Sheng J, Tran PN, et al. Assessment of an *in silico* mechanistic model for proarrhythmia risk prediction under the CiPA initiative. *Clin Pharmacol Ther* 2019;105:466-475. [PUBMED](#) | [CROSSREF](#)
9. Payne RA, Avery AJ. Polypharmacy: one of the greatest prescribing challenges in general practice. *Br J Gen Pract* 2011;61:83-84. [PUBMED](#) | [CROSSREF](#)
10. European Medicines Agency. Guideline on the investigation of drug interactions. London: European Medicines Agency; 2012.
11. Redfern WS, Carlsson L, Davis AS, Lynch WG, MacKenzie I, Palethorpe S, et al. Relationships between preclinical cardiac electrophysiology, clinical QT interval prolongation and torsade de pointes for a broad range of drugs: evidence for a provisional safety margin in drug development. *Cardiovasc Res* 2003;58:32-45. [PUBMED](#) | [CROSSREF](#)
12. Hancox JC, McPate MJ, El Harchi A, Zhang YH. The hERG potassium channel and hERG screening for drug-induced torsades de pointes. *Pharmacol Ther* 2008;119:118-132. [PUBMED](#) | [CROSSREF](#)
13. McPate MJ, Duncan RS, Hancox JC, Witchel HJ. Pharmacology of the short QT syndrome N588K-hERG K⁺ channel mutation: differential impact on selected class I and class III antiarrhythmic drugs. *Br J Pharmacol* 2008;155:957-966. [PUBMED](#) | [CROSSREF](#)
14. Wiśniowska B, Lisowski B, Kulig M, Polak S. Drug interaction at hERG channel: *in vitro* assessment of the electrophysiological consequences of drug combinations and comparison against theoretical models. *J Appl Toxicol* 2018;38:450-458. [PUBMED](#) | [CROSSREF](#)
15. Delaunois A, Abernathy M, Anderson WD, Beattie KA, Chaudhary KW, Coulot J, et al. Applying the CiPA approach to evaluate cardiac proarrhythmia risk of some antimalarials used off-label in the first wave of COVID-19. *Clin Transl Sci* 2021;14:1133-1146. [PUBMED](#) | [CROSSREF](#)
16. Montnach J, Baró I, Charpentier F, De Waard M, Loussouarn G. Modelling sudden cardiac death risks factors in patients with coronavirus disease of 2019: the hydroxychloroquine and azithromycin case. *Europace* 2021;23:1124-1133. [PUBMED](#) | [CROSSREF](#)
17. Varshneya M, Irurzun-Arana I, Campana C, Dariolli R, Gutierrez A, Pullinger TK, et al. Investigational treatments for COVID-19 may increase ventricular arrhythmia risk through drug interactions. *CPT Pharmacometrics Syst Pharmacol* 2021;10:100-107. [PUBMED](#) | [CROSSREF](#)
18. Whittaker DG, Capel RA, Hendrix M, Chan XHS, Herring N, White NJ, et al. Cardiac TdP risk stratification modelling of anti-infective compounds including chloroquine and hydroxychloroquine. *R Soc Open Sci* 2021;8:210235. [PUBMED](#) | [CROSSREF](#)
19. Reiffel JA, Robinson VM, Kowey PR. Perspective on antiarrhythmic drug combinations. *Am J Cardiol* 2023;192:116-123. [PUBMED](#) | [CROSSREF](#)
20. Coumel P, Chouty F, Slama R. Logic and empiricism in the selection of antiarrhythmic agents. The role of drug combinations. *Drugs* 1985;29 Suppl 4:68-76. [PUBMED](#) | [CROSSREF](#)

21. Reiffel JA. Reduced-dose antiarrhythmic drugs: valuable or valueless? *J Innov Card Rhythm Manag* 2020;11:4063-4067. [PUBMED](#) | [CROSSREF](#)
22. Qauli AI, Marcellinus A, Setiawan MA, Zain AFN, Pinandito AM, Lim KM. *In silico* assessment on TdP risks of drug combinations under CiPA paradigm. *Sci Rep* 2023;13:2924. [PUBMED](#) | [CROSSREF](#)
23. Rea F, Corrao G, Merlino L, Mancia G. Early cardiovascular protection by initial two-drug fixed-dose combination treatment vs. monotherapy in hypertension. *Eur Heart J* 2018;39:3654-3661. [PUBMED](#) | [CROSSREF](#)
24. Schmieder RE, Wassmann S, Predel HG, Weisser B, Blettenberg J, Gillissen A, et al. Improved persistence to medication, decreased cardiovascular events and reduced all-cause mortality in hypertensive patients with use of single-pill combinations: results from the START-Study. *Hypertension* 2023;80:1127-1135. [PUBMED](#) | [CROSSREF](#)
25. Afzal MR, Savona S, Mohamed O, Mohamed-Osman A, Kalbfleisch SJ. Hypertension and arrhythmias. *Heart Fail Clin* 2019;15:543-550. [PUBMED](#) | [CROSSREF](#)
26. Egan BM, Zhao Y, Axon RN. US trends in prevalence, awareness, treatment, and control of hypertension, 1988-2008. *JAMA* 2010;303:2043-2050. [PUBMED](#) | [CROSSREF](#)
27. Mancia G, Fagard R, Narkiewicz K, Redon J, Zanchetti A, Böhm M, et al. 2013 ESH/ESC Guidelines for the management of arterial hypertension: the Task Force for the management of arterial hypertension of the European Society of Hypertension (ESH) and of the European Society of Cardiology (ESC). *Eur Heart J* 2013;34:2159-2219. [PUBMED](#) | [CROSSREF](#)
28. Bliss CI. The toxicity of poisons applied jointly. *Ann Appl Biol* 1939;26:585-615. [CROSSREF](#)
29. O'Hara T, Virág L, Varró A, Rudy Y. Simulation of the undiseased human cardiac ventricular action potential: model formulation and experimental validation. *PLOS Comput Biol* 2011;7:e1002061. [PUBMED](#) | [CROSSREF](#)
30. Li Z, Dutta S, Sheng J, Tran PN, Wu W, Chang K, et al. Improving the *in silico* assessment of proarrhythmia risk by combining hERG (human ether-à-go-go-related gene) channel-drug binding kinetics and multichannel pharmacology. *Circ Arrhythm Electrophysiol* 2017;10:e004628. [PUBMED](#) | [CROSSREF](#)
31. Tomek J, Bueno-Orovio A, Passini E, Zhou X, Mincholé A, Britton O, et al. Development, calibration, and validation of a novel human ventricular myocyte model in health, disease, and drug block. *eLife* 2019;8:e48890. [PUBMED](#) | [CROSSREF](#)
32. Ivanov SM, Lagunin AA, Filimonov DA, Poroikov VV. Computer prediction of adverse drug effects on the cardiovascular system. *Pharm Chem J* 2018;52:758-762. [CROSSREF](#)
33. Ivanov S, Lagunin A, Filimonov D, Poroikov V. Assessment of the cardiovascular adverse effects of drug-drug interactions through a combined analysis of spontaneous reports and predicted drug-target interactions. *PLOS Comput Biol* 2019;15:e1006851. [PUBMED](#) | [CROSSREF](#)
34. Wicha SG, Chen C, Clewe O, Simonsson USH. A general pharmacodynamic interaction model identifies perpetrators and victims in drug interactions. *Nat Commun* 2017;8:2129. [PUBMED](#) | [CROSSREF](#)
35. Liu Q, Yin X, Languino LR, Altieri DC. Evaluation of drug combination effect using a Bliss independence dose-response surface model. *Stat Biopharm Res* 2018;10:112-122. [PUBMED](#) | [CROSSREF](#)
36. Benet LZ. Chapter 2. Pharmacokinetics: the dynamics of drug absorption, distribution, metabolism, and elimination. In: Hilal-Dandan R, Brunton LL (eds). *Goodman and Gilman's the pharmacological basis of therapeutics*. 2nd ed. New York (NY): McGraw-Hill Companies, Inc.; 2016.
37. Maisel AS, Motulsky HJ, Insel PA. Hypotension after quinidine plus verapamil - possible additive competition at alpha-adrenergic receptors. *N Engl J Med* 1985;312:167-170. [CROSSREF](#)
38. Lavoie R, Blevins RD, Rubenfire M, Edwards DJ. The effect of verapamil on quinidine pharmacokinetics in man. *Drug Intell Clin Pharm* 1986;20:457.
39. Trohman RG, Estes DM, Castellanos A, Palomo AR, Myerburg RJ, Kessler KM. Increased quinidine plasma concentrations during administration of verapamil: a new quinidine-verapamil interaction. *Am J Cardiol* 1986;57:706-707. [PUBMED](#) | [CROSSREF](#)
40. Laganière S, Davies RF, Carignan G, Foris K, Goernert L, Carrier K, et al. Pharmacokinetic and pharmacodynamic interactions between diltiazem and quinidine. *Clin Pharmacol Ther* 1996;60:255-264. [PUBMED](#) | [CROSSREF](#)
41. Matera MG, De Santis D, Vacca C, Fici F, Romano AR, Marrazzo R, et al. Quinidine-diltiazem: pharmacokinetic interaction in humans. *Curr Ther Res Clin Exp* 1986;40:653-656.
42. Lenz TL, Hilleman DE. Dofetilide, a new class III antiarrhythmic agent. *Pharmacotherapy* 2000;20:776-786. [PUBMED](#) | [CROSSREF](#)
43. Broly F, Vandamme N, Caron J, Libersa C, Lhermitte M. Single-dose quinidine treatment inhibits mexiletine oxidation in extensive metabolizers of debrisoquine. *Life Sci* 1991;48:PL123-PL128. [PUBMED](#) | [CROSSREF](#)

44. Michalets EL. Update: clinically significant cytochrome P-450 drug interactions. *Pharmacotherapy* 1998;18:84-112. [PUBMED](#) | [CROSSREF](#)
45. Fuadah YN, Qauli AI, Marcellinus A, Pramudito MA, Lim KM. Machine learning approach to evaluate TdP risk of drugs using cardiac electrophysiological model including inter-individual variability. *Front Physiol* 2023;14:1266084. [PUBMED](#) | [CROSSREF](#)